

Exciton localization in $\text{Mg}_x\text{Zn}_y\text{Cd}_{1-x-y}\text{Se}$ alloy

O. Maksimov^{*1}, W. H. Wang¹, N. Samarth¹, M. Muñoz², and M. C. Tamargo²

¹ Department of Physics, Pennsylvania State University, University Park, PA 16802, USA

² Department of Chemistry, City College of New York, New York, NY 10031, USA

Received 22 September 2003, revised 15 October 2003, accepted 25 November 2003

Published online 12 February 2004

PACS 71.35.-y, 78.30.Fs, 78.40.Fy, 78.55.Et

We report photoluminescence and reflectivity measurements of $\text{Mg}_x\text{Zn}_y\text{Cd}_{1-x-y}\text{Se}$ epitaxial layers ($0 < x < 0.53$) grown by molecular beam epitaxy on InP (100) substrates. Significant emission line broadening, increase in activation energy and Stokes shift are monitored with increasing Mg content. For $\text{Mg}_x\text{Cd}_y\text{Zn}_{1-x-y}\text{Se}$ samples with large Mg content ($x > 0.3$), we observe an anomalous temperature dependence of both the emission energy and line broadening. This behavior is assigned to the emission from localized states. Different mechanisms of carrier localization are discussed and exciton localization on statistical CdSe clusters is proposed to be the most likely one.

© 2004 WILEY-VCH Verlag GmbH & Co. KGaA, Weinheim

1 Introduction Although substantial success has been achieved in the development and production of $\text{Al}_x\text{In}_y\text{Ga}_{1-x-y}\text{N}$ -based light emitting and laser diodes (LEDs and LDs) that operate in the ultraviolet, violet, and blue spectral range, it has been more challenging to produce long-life devices operating at longer visible wavelengths due to the high threshold current density required for lasing [1]. Since $\text{Al}_x\text{Ga}_y\text{In}_{1-x-y}\text{P}$ -based LDs operate only at wavelengths longer than 600 nm, there is a spectral gap in the green-yellow region (530–590 nm) that is directly relevant for emerging technologies such as the use of plastic optical fibers that require green lasers to achieve the lowest attenuation coefficient. Together with the recent improvements in the degradation stability, this revives interest in ZnSe-based LDs that can potentially cover the whole green spectral region (490–590 nm) [2].

The $\text{Mg}_x\text{Zn}_y\text{Cd}_{1-x-y}\text{Se}$ material system is particularly interesting since it can be used to produce light emitters operating in red, green, and blue regions of the visible spectrum [3]. For instance, $\text{Mg}_x\text{Zn}_y\text{Cd}_{1-x-y}\text{Se}$ -based current injected lasers operating at 560 nm were reported recently [4]. However, to fully exploit this material system, it is important to understand the light emission mechanism in the alloy.

In this paper, we report photoluminescence (PL) and reflectivity measurements of high-quality $\text{Mg}_x\text{Zn}_y\text{Cd}_{1-x-y}\text{Se}$ ($0 < x < 0.53$) epilayers grown by molecular beam epitaxy (MBE) on InP substrates. While the low-temperature PL spectra of $\text{Zn}_{0.5}\text{Cd}_{0.5}\text{Se}$ epilayers are dominated by near band edge emission characterized by narrow asymmetric lines with a high-energy tail, we find that PL spectra of $\text{Mg}_x\text{Zn}_y\text{Cd}_{1-x-y}\text{Se}$ epilayers are dominated by broad asymmetric lines with a low energy tail. We have studied the behaviour of the emission lines as a function of excitation intensity and temperature, revealing the excitonic origin of the emission. As the Mg content is increased, we find a substantial emission line broadening, an increase in activation energy, and a large Stokes shift. For $\text{Mg}_x\text{Cd}_y\text{Zn}_{1-x-y}\text{Se}$ with large Mg content ($x > 0.3$), we observe an anomalous temperature dependence (“S-shaped” emission energy shift and emission line broadening). We interpret this unusual behaviour in terms of exciton localization in $\text{Mg}_x\text{Zn}_y\text{Cd}_{1-x-y}\text{Se}$ alloys with high Mg content ($x > 0.3$) and speculate that exciton localization on statistical clusters is responsible for the observations.

* Corresponding author: e-mail: Maksimov@netzero.net, Phone: +1 814 863 9514, Fax: +1 814 865 3604

2 Experimental details All samples were grown by MBE on semi-insulating InP (100) substrates under the growth conditions described elsewhere [3]. The composition of the ternary $\text{Zn}_y\text{Cd}_{1-x}\text{Se}$ alloy was calculated from the lattice constant measured using a double-crystal X-ray diffraction (DCXRD) system, assuming a linear dependence of lattice constant on the alloy composition (Vegard's law). The composition of the quaternary $\text{Mg}_x\text{Zn}_y\text{Cd}_{1-x-y}\text{Se}$ alloy was determined by the combination of lattice constant and bandgap energy data [5]. PL measurements were performed in a liquid He continuous flow cryostat in the temperature range from 4.2 K to 300 K. Excitation was provided by the 325-nm line of a He-Cd laser. Reflectivity measurements were performed in the same cryostat using a 200-W Hg lamp.

3 Results and discussion Figure 1 shows PL spectra (dotted lines) at 4.2 K for $\text{Mg}_x\text{Zn}_y\text{Cd}_{1-x-y}\text{Se}$ epilayers with $x = 0, 0.25, 0.31, 0.34,$ and 0.53 . The spectra are dominated by near band edge emission lines and no deep level emission is observed, indicating high material quality. With increasing Mg content, the data show a significant broadening of the emission line (from 6 meV for $\text{Zn}_{0.5}\text{Cd}_{0.5}\text{Se}$ to 65 meV for $\text{Mg}_{0.53}\text{Zn}_{0.27}\text{Cd}_{0.2}\text{Se}$). This broadening is accompanied by a change in lineshape. The emission from $\text{Zn}_{0.5}\text{Cd}_{0.5}\text{Se}$ is dominated by a sharp asymmetric line with a high-energy tail. In contrast, the emission from $\text{Mg}_x\text{Zn}_y\text{Cd}_{1-x-y}\text{Se}$ ($x \sim 0.25$) has a symmetric Gaussian shape and is significantly broader due to the increase in the alloy disorder. For higher Mg content ($x > 0.3$), the emission lines have asymmetric line shapes with a low-energy tail, possibly arising from the formation of an exponential tail of localized states.

Reflectivity spectra (solid lines) at 4.2 K for $\text{Zn}_{0.5}\text{Cd}_{0.5}\text{Se}$ and $\text{Mg}_{0.53}\text{Zn}_{0.27}\text{Cd}_{0.2}\text{Se}$ epilayers are also shown in Figure 1. The quenching of Fabry-Perot oscillations in the reflectivity spectrum corresponds to the onset of interband absorption and is identified as the $\Gamma \rightarrow \Gamma$ direct band gap transition. An increase in the Stokes shift from ~ 10 meV for $\text{Zn}_{0.5}\text{Cd}_{0.5}\text{Se}$ to ~ 90 meV for $\text{Mg}_{0.53}\text{Zn}_{0.27}\text{Cd}_{0.2}\text{Se}$ is evident.

We studied the dependence of the emission on the excitation laser intensity to elucidate the origin of the emission lines. Excitation laser intensity was varied over three order of magnitude and a linear dependence of the PL emission intensity with a slope near unity was obtained. Also, no shift of the emission energy was observed. This behaviour is consistent with the excitonic origin of emission.

Figure 2 shows the dependence of the PL emission energy on temperature (solid circles). In general, the emission energy follows the temperature dependence of the band gap shrinkage described by Bose-Einstein type relationship [6]: $E_g(T) = E_g(0) - 2a_B/(\exp(\theta/T) - 1)$, where $E_g(T)$ is the band-gap transition energy at the temperature T , a_B represents the strength of the average electron-phonon interaction, and θ corresponds to the average phonon temperature.

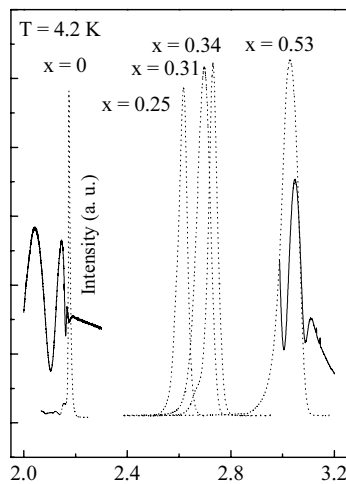


Fig. 1 Low temperature photoluminescence (dotted lines) and reflectivity (solid lines) spectra of $\text{Mg}_x\text{Zn}_y\text{Cd}_{1-x-y}\text{Se}$ epilayers with different Mg content (x).

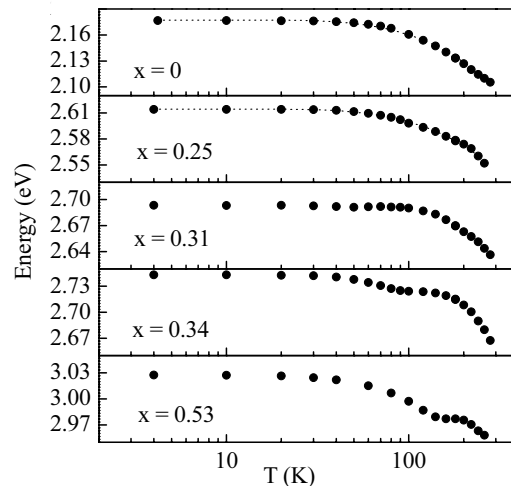


Fig. 2 Temperature dependence of the emission energy. Symbols correspond to the experimental data and the dotted lines are the fits using Bose-Einstein type relationship.

At small values of x ($x \leq 0.3$), the temperature-dependent PL peak shift is consistent with the estimated decrease in energy. The experimental data are well fitted to the Bose-Einstein equation with $a_B = 21$ meV, $\theta = 124$ K and $a_B = 24$ meV, $\theta = 169$ K for the samples with 0 and 25% of Mg, respectively (dotted lines). In striking contrast, for $\text{Mg}_x\text{Zn}_y\text{Cd}_{1-x-y}\text{Se}$ epilayers with larger x values, the temperature-dependent PL peak shift does not follow the typical temperature dependence of the energy gap shrinkage. Instead, we find a non-monotonic (“S-shaped”) emission shift with increasing temperature. The emission energy decreases when temperature is below T_1 (50 K for $x = 0.31$, 90 K for $x = 0.34$, 140 K for $x = 0.53$), slightly increases when temperature is below T_2 (90 K for $x = 0.31$, 140 K for $x = 0.34$, 200K for $x = 0.53$), and then starts to decrease again. Temperatures corresponding to the changes in the behaviour (T_1 and T_2) depend on the composition and increase with Mg content. This type of behaviour is characteristic for the localized exciton emission and can be explained by the increase in localization energy [7].

Figure 3 shows the dependence of the full width at half maximum (FWHM) of the PL emission line on temperature (solid circles). The measured luminescence line width is a sum of an inhomogeneous part (Γ_i) that is due to the extrinsic effects (dislocations, composition fluctuations, alloy scattering, and electron-electron interactions) and a temperature-dependent homogeneous part (Γ_h). At low temperatures, the homogeneous component is dominated by scattering of acoustical phonons (AC). As the temperature increases, the longitudinal optical (LO) phonon scattering becomes dominant due to the increase of phonon population.

The temperature-dependent emission line broadening for $\text{Mg}_x\text{Zn}_y\text{Cd}_{1-x-y}\text{Se}$ epilayers with small x value ($x \leq 0.3$) is consistent with the model: a slow broadening due to AC scattering at low temperatures is followed by a fast broadening due to the LO scattering at higher temperatures. The temperature-dependent emission line broadening for $\text{Mg}_x\text{Zn}_y\text{Cd}_{1-x-y}\text{Se}$ epilayers with larger x values shows an anomalous “S-shaped” broadening. An increase in FWHM of the emission line at low temperatures is followed by the decrease at moderate temperatures and further increase at higher temperatures.

Figure 4 shows an Arrhenius plot of the normalized PL intensities as a function of temperature (solid circles). The PL intensity decreases with increasing temperature, indicating the presence of non-radiative recombination centres. The experimental data is fitted to a formula involving one non-radiative recombination process (dotted lines) [8]: $I(T) = 1/(1 + (P_{NR}/P_R) \exp(-E_A/k_B T))$, where P_{NR}/P_R is the ratio of the non-radiative to radiative recombination probability, T is the temperature, k_B is the Boltzmann’s constant, and E_A is the activation energy. An increase in the thermal activation energy with increasing Mg content (from 24 meV for $\text{Zn}_{0.5}\text{Cd}_{0.5}\text{Se}$ to 108 meV for $\text{Mg}_{0.53}\text{Zn}_{0.27}\text{Cd}_{0.2}\text{Se}$) is observed. This increase is in a good agreement with the increase in the Stokes shift between the PL peak energy and the bandgap measured through reflectivity measurements. It should be noted that E_A reported for $\text{Zn}_{0.5}\text{Cd}_{0.5}\text{Se}$ is close to the exciton binding energy previously reported for $\text{Zn}_{0.53}\text{Cd}_{0.47}\text{Se}$ (20 meV) [9]. Therefore, the decrease in the PL intensity is due to the thermal activation of localized excitons to free carriers and their further nonradiative recombination.

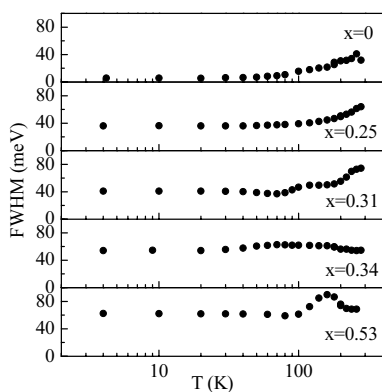


Fig. 3 Temperature dependence of the line width of the emission. Symbols correspond to the experimental data. Dotted lines correspond to the experimental data.

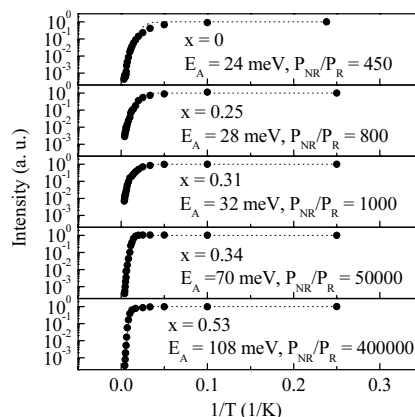


Fig. 4 Arrhenius plot of the emission intensity vs inverse temperature. Symbols correspond to the experimental data and the dotted lines are the fits using one-step non-radiative recombination model.

These results suggest that exciton localization occurs in $\text{Mg}_x\text{Zn}_y\text{Cd}_{1-x-y}\text{Se}$ alloy with large Mg content and localized states with energies 100 meV below band gap are forming in $\text{Mg}_{0.53}\text{Zn}_{0.27}\text{Cd}_{0.2}\text{Se}$. Good crystalline quality of the epilayers was verified by DCXRD measurements and no presence of phase separation or spontaneous alloy ordering that can be responsible for carrier localization was observed.

Carrier localization can occur in high crystalline quality homogeneous alloy due to the random potential fluctuations [7]. Isoelectronic traps or clusters of the low-bandgap component of the alloy (CdSe) can serve as localization centres. The mechanism of carrier localization depends on the ratio between the depth of the well created by CdSe (Δ) and critical energy of perturbation (E_{cr}) defined as [10]: $E_{\text{cr}} = \hbar^2/m_{\text{eff}}a^2$, where m_{eff} is the carrier effective mass and a is a spatial size of the well and is on the order of interatomic distance. Using the data reported for CdSe ($m_{\text{eff}} = 0.45m_0$ for heavy holes, $m_{\text{eff}} = 0.11m_0$ for electrons, and $a = 3.0 \text{ \AA}$) [11], we estimate that E_{cr} is $\sim 1.875 \text{ eV}$ for holes and is significantly larger for electrons due to their smaller effective mass. Since most of the band discontinuity in the $\text{Mg}_x\text{Zn}_y\text{Cd}_{1-x-y}\text{Se}/\text{CdSe}$ system is in the conduction band ($\Delta E_c/\Delta E_g \sim 0.8$) [12], and CdSe band gap is $\sim 1.77 \text{ eV}$, we calculate Δ : $\Delta \approx \Delta E_c/\Delta E_g \cdot (E_g^{(\text{MgZnCdSe})} - E_g^{(\text{CdSe})})$. Δ increases from 190 meV to 260 meV when x increases from 0.3 to 0.53. Since E_{cr} exceeds Δ , formation of isoelectronic traps is not likely. However, Δ is large enough to allow hole localization on statistical CdSe clusters involving a few Cd atoms occupying the near-neighbour sites in the crystal lattice. Localized holes can bind electrons forming localized excitons. Then, an asymmetric shape of the $\text{Mg}_x\text{Zn}_y\text{Cd}_{1-x-y}\text{Se}$ ($x > 0.3$) emission line is due to the sum of the emission lines from clusters with different emission energies. ‘‘S-shaped’’ emission energy shift and emission line broadening are due to thermalization of localized excitons with different activation energies. Their activation, followed by the depletion with increasing temperature, briefly dominates the overall downward trend of the band gap. It also causes narrowing of the emission line at higher temperatures. Finally, increase in the Stokes shift and activation energy with increasing Mg content is due to the increase in the band gap energy of the host alloy as well as to the decrease in the potential fluctuations outside the clusters that prevents tunnelling energy transfer between them.

4 Conclusion We have investigated optical properties of $\text{Mg}_x\text{Zn}_y\text{Cd}_{1-x-y}\text{Se}$ epilayers ($0 \leq x \leq 0.53$) via PL and reflectivity spectroscopy. An anomalous temperature-induced PL emission behaviour for $\text{Mg}_x\text{Zn}_y\text{Cd}_{1-x-y}\text{Se}$ alloy with high Mg content ($x > 0.3$) (an ‘S-shaped’ PL peak energy shift and an ‘S-shaped’ PL emission line broadening) was observed. The deviation from the typical temperature dependence and the temperature range in which it occurred was increasing with the Mg content. A significant increase in the activation energy of the PL emission and Stokes shift were also observed. This behaviour indicates carrier localization in $\text{Mg}_x\text{Zn}_y\text{Cd}_{1-x-y}\text{Se}$ alloy ($x > 0.3$). Possible mechanisms of carrier localization were discussed and exciton localization on statistical clusters was proposed to be the most possible.

References

- [1] S. Nakamura, M. Senoh, S. Nagahama, N. Iwasa, T. Matsushita, and T. Mukai, *Appl. Phys. Lett.* **76**, 22 (2000).
- [2] S. V. Ivanov, *phys. stat. sol. (a)* **192**, 157 (2002).
- [3] M. C. Tamargo, S. P. Guo, O. Maksimov, Y. C. Chen, F. C. Peiris, and J. K. Furdyna, *J. Cryst. Growth* **227**, 710 (2001).
- [4] S. B. Che, I. Nomura, A. Kikuchi, and K. Kishino, *Appl. Phys. Lett.* **81**, 972 (2002).
- [5] O. Maksimov, S. P. Guo, M. C. Tamargo, F. C. Peiris, and J. K. Furdyna, *J. Appl. Phys.* **89**, 2202 (2001).
- [6] L. Viña, S. Logothetidis, and M. Cardona, *Phys. Rev. B* **30**, 1979 (1984).
- [7] Y. Kawakami, M. Funato, S. Fujita, Y. Yamada, and Y. Masumoto, *Phys. Rev. B* **50**, 14655 (1990).
- [8] J. D. Lambkin, L. Considine, S. Walsh, G. M. Oconnor, C. J. McDonagh, and T. J. Glynn, *Appl. Phys. Lett.* **65**, 3451 (1994).
- [9] T. Holden, P. Ram, F. H. Pollak, J. L. Freeouf, and M. C. Tamargo, *Phys. Rev. B* **56**, 4037 (1997).
- [10] S. Permogorov, A. Klochikhin, and A. Reznitsky, *J. Lumin.* **100**, 243 (2002).
- [11] I. Hernandez-Calderon, in: *II–VI Semiconductor Materials and Their Applications*, edited by M. C. Tamargo (Taylor and Francis, New York, 2002).
- [12] M. Muñoz, H. Lu, X. Zhou, M. C. Tamargo, and F. H. Pollak, *Appl. Phys. Lett.* **83**, 1995 (2003).